

Images from the Mind: BCI image evolution based on RSVP of polygon primitives

L. F. Seoane^{1,2,3}, S. Gabler³, and B. Blankertz^{3,4,5}

¹ICREA-Complex Systems Lab, Universitat Pompeu Fabra, Dr. Aiguader 80, 08003 Barcelona, Spain.

²Institut de Biologia Evolutiva, CSIC-UPF, Psg Barceloneta, Barcelona Spain.

³Bernstein Center for Computational Neuroscience, Technische Universität Berlin, Germany.

⁴Neurotechnology Group, Berlin Institute of Technology, Berlin, Germany.

⁵Bernstein Focus: Neurotechnology, Berlin, Germany.

May 16, 2022

Abstract

This paper provides a proof of concept for an EEG-based evolution of a visual image which is on a user's mind. Our approach is based on the Rapid Serial Visual Presentation (RSVP) of polygon primitives and Brain-Computer Interface (BCI) technology. The presentation of polygons that contribute to build a target image (because they match the shape and/or color of the target) trigger attention-related EEG patterns. Accordingly, these target primitives can be determined using BCI classification of Event-Related Potentials (ERPs). They are then accumulated in the display until a satisfactory reconstruction is reached. Each selection step had an average classification accuracy of about 75%. An in-depth investigation suggests that most of the misclassification were not misinterpretations of the BCI concerning the users' intent, but rather stemmed from the fact that the users tried to select different polygons than the experimenter wanted them to select. Open problems and alternatives to develop a practical BCI-based image reconstruction application are discussed.

1 Introduction

We introduce a Brain-Computer Interface (BCI) application based on Rapid Serial Visual Presentation (RSVP) of polygon primitives for image reconstruction. Our paradigm relies on the decomposition of a collection of images (figure 1) into a set of approximate constituent parts (polygon primitives). These primitives are presented to the experimental subjects in bursts. Event Related Potentials (ERPs) associated to the oddball paradigm [1, 2] are used as EEG correlates to detect those pieces that contribute to the reconstruction of the target image (which is on the user's mind) in an incremental fashion. The operational basis (RSVP) had already been employed for BCI-based gaze-independent spellers [3, 4, 5]. The results presented in this paper invite us to be optimistic about this new paradigm for BCI image reconstruction. More experiments should be carried out to expand the design outside the chosen collection of images, ideally moving towards a free painting device. Some ideas are proposed based on the outcome of the current work. The experiments also suggest ways to increase the reliability, speed, and accuracy of the

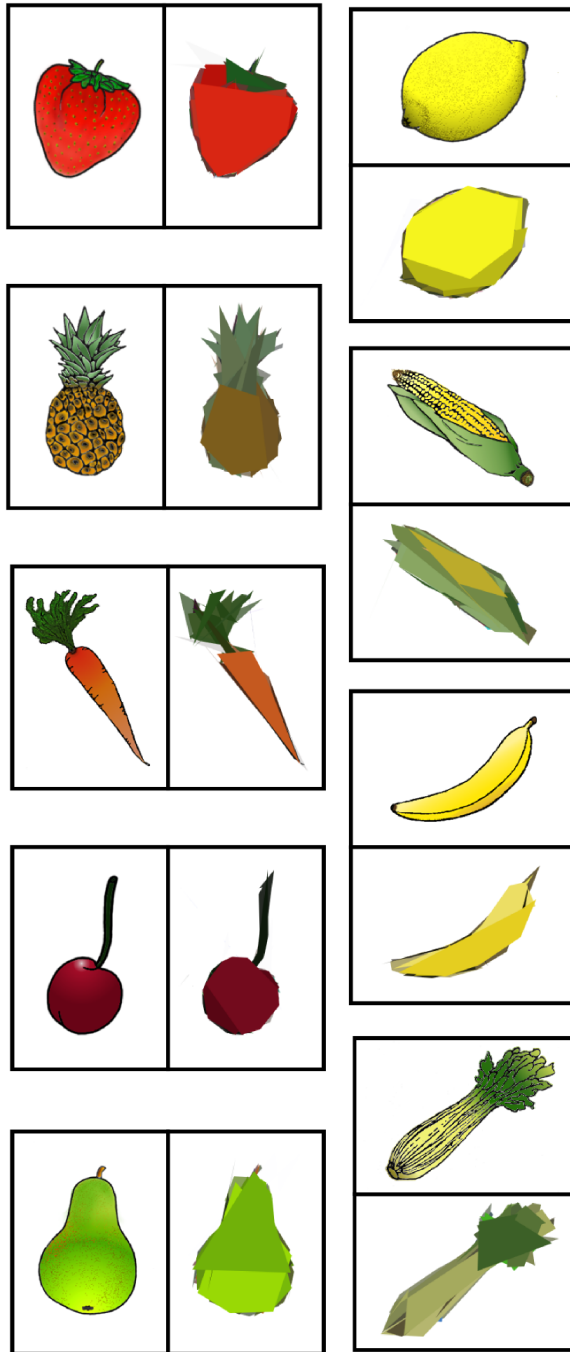


Figure 1: **Images selected as BCI reconstruction targets.** The chosen images comprise very basic and recognizable shapes with bright colors. Besides, some of the drawings present relatively small details that become important as the reconstruction advances. The polygon decompositions obtained for each image are also shown correctly assembled.

current framework.

Our work draws important inspiration from recent advances in Cortically-Coupled Computer Vision (C3Vision) [6, 7, 8] where human vision is enhanced through an efficient data mining of EEG patterns while stimuli are presented. Such an approach has shown how the search for target images among a large data set can be boosted, and how it is possible to speed up the localization of salient details from within a large image [9, 10]. Even further improvement can be achieved with a *closed loop* philosophy [11, 12] in which human vision and EEG are not only coupled, but engage in a cycle where the artificial intelligence behind the EEG-based classifiers offers feedback in real time. These seminal studies provide interesting insights about the capabilities of such BCIs and suggest that the limits of our own design could be pushed further.

In [13] we find an early approach closer to the line of research that we pursue. Physiological states – including EEG and indicators such as ventilation, heart rate, and others – are correlated to ‘positive’ and ‘negative’ feelings elicited by visual stimuli. The ability to prompt the same positive reactions are then used as fitness functions for new, randomly generated images that evolve by means of a genetic algorithm. The decisions based on these cues are compared offline to the deliberate choices made by the experimental subjects who should decide what images were more *artsy*. Letting aside the fulfillment of the global goal (evolving art), the setup in [13] reproduces the choices made by the individuals with moderate success (61% accuracy).

While in [13] the authors intend to explore the undetermined space of art, Shamlo and Makeig [14] sketch a procedure to evolve towards a definite target image. Bursts of randomly generated drawings are presented to the subjects, whose EEGs are recorded. A burst might or might not contain a target image that resembles “two eyes”. Besides the recording of neural activity, the subjects must press a button after each burst to indicate if the target has been consciously spotted out. EEG patterns are extracted that correlate with the presence of the target image during a burst. The authors focus on a very elaborate processing of the data during a posterior offline anal-

ysis. Using ten fold cross-validation on single trial data, very high accuracy is obtained (up to 0.98 area under ROC curve).

Following these promising results, the authors in [14] propose to use the EEG activity during bursts to evolve images. Available software [15] accepts user-provided images and attempts to evolve them towards a desired target picture. Random mutations and crossover are applied on the original feed to generate newer candidates. In the standard approach, the user chooses among the new candidates those that fall closer to an arbitrary goal (e.g. “two eyes” in [14]). This manual procedure results cumbersome. Using EEG features to identify what images should be fed to the algorithm could speed up the evolutionary process. Unluckily, such interesting possibility is only suggested in [14] based on the good performance of the EEG-driven classification task. Actual experiments should be implemented to test the complete BCI-evolutionary-algorithm loop suggested in [14].

The *P300-Brain Painting* BCI [16, 17, 18] inspired by the early P300-Speller BCIs [19] is the device closer to ours in terms of goals and performance. These works use a BCI to interface with more standard bit map processing software. Using the oddball paradigm; colors, shapes, and a variety of tools are selected from a matrix as rows and columns are highlighted. The selected operators modify an existing canvas in a similar way that a mouse interface would do. In [18] this BCI was evaluated in healthy subjects and ALS patients finding, for certain design specifications, performances comparable to those of the equivalent matrix speller. The P300-Brain Painting device offers room for improvement in many aspects, but the insights from those works are more complicated to translate to ours due to the important differences in implementation. We research two different – albeit similar in purpose – design.

The paradigm explored in [13] relies on physiological signals. This slows down the interface drastically, as tens of seconds are necessary to collect reliable data. But the approach in [14] and others [11, 12] set an interesting precedent for our BCI given the high rate at which stimuli are presented (up to 12 Hz). We chose more conservative rates (~ 3 Hz) for the proof of concept introduced here. Another

crucial difference between most examples in the literature and ours is that we proceed bottom-up to reconstruct a set of images: our stimuli are polygon primitives that might resemble smaller details of a target image, this allows for a finer grained reconstruction than those in [13, 14]. In there, each stimulus is a whole picture and targets are based on broader features such as the existence of two eyes. This will be important if we wanted to extrapolate the technical setup (mainly the stimulus rate) to our design. Besides, in our experiments actual image reconstructions were undertaken, thus we offer the first serious test of this novel and promising BCI paradigm.

The paper is organized as follows: In section 2 the proposed BCI is described along with the experimental and data analysis details. In section 3 the results are summarized. We close with a discussion of these results in section 4, where future lines or research are proposed together with possible improvements and alternatives to the current design. Appendix A includes a description of the choices made regarding the preprocessing of the images and the experimental setup. This is compared with similar BCI schemes that inspired the research. Appendix B analyzes in detail an anomaly found in some image reconstructions.

2 Methods

2.1 Participants

Ten participants (five women and five men, ages ranging from early twenties to early thirties) took part in the experiment on a voluntary, non rewarded basis. One of the subjects was associated to the BCI research group and this subjects and other two had previous experiences with BCI experiments. The rest of the subjects were naïve with respect to BCI technologies. All of them had normal or corrected to normal vision and did not report any health issues along the experiment.

2.2 Apparatus

EEG was recorded at 1000 Hz using BrainAmp amplifiers and an actiCap active electrode system with 63 channels (both by Brain Products, Munich, Germany). The electrodes used were Fp1,2, AF3,4,7,8, Fz, F1-10, FCz, FC1-6, FT7,8, Cz, C1-6, T7,8, CPz, CP1-6, TP7,8, Pz, P1-10, POz, PO3,4,7,8, Oz, O1,2. All electrodes were referenced to the left mastoid using a forehead ground. For offline analyses electrodes were re-referenced to linked mastoids. All the impedances were kept below 10 k Ω .

Stimuli were presented on a 24" TFT screen with a refresh rate of 60 Hz and a resolution of 1920 \times 1200 px². The experiment was implemented in Python using the open-source BCI framework Pyff [20] with Pygame [21] and Vision-Egg [22]. Data analysis and classification were performed with MATLAB (The MatlabWorks, Natick, MA, USA) using an in-house BCI toolbox (www.bbci.de/toolbox).

2.3 Design and procedure

The design of the experiment includes a pre-processing of the images to extract the primitives that are shown during RSVP bursts. Important choices regarding stimulus presentation were also made. Because we explore a novel paradigm, almost any design feature is open to debate. In the following, we report the actual choices made for the experiment. For an introduction and discussion of the other possibilities the reader is referred to appendix A.

2.3.1 Preprocessing of target images

The 9 drawings of fruits and vegetables collected in figure 1 were chosen as potential targets for reconstruction from the revised Snodgrass and Vanderwart's object database [23]. They are easily recognizable, present bright, plain colors, and combine basic shapes with some minor details – such as the stalk of the cherry – that could act as landmarks during a reconstruction task. They are always displayed upon a blank background.

Similar to the role played by letters in RSVP spellers [3, 4, 5], we need nuclear units that constitute

stimuli during the bursts of our BCI paradigm. These stimuli must be able to reconstruct the target images as they accumulate in the screen. We submitted the chosen images to a preprocessing step during which a genetic algorithm [24] extracted a series of primitives (polygons) that approximated the drawings up to a satisfactory degree (final product shown in figure 1). We refer to these primitives throughout the text as the *polygon decomposition* of each of the targets. A brief description of the genetic algorithm is found in the appendix A.1. The actual code that we used and the values of different parameters employed in our implementation can be found in a public repository [25].

The resulting decompositions contain between 4 and 10 polygons (with 6.7 on average) depending on the target drawing. We restricted polygons to have between 3 and 7 vertexes and solid colors – i.e. no transparency was allowed. Polygons are overlaid upon a blank background and upon each other, thus their depth matters for the reconstruction task.

The *fitness* function used as a selection criterion by the genetic algorithm (see appendix A.1) is a pixel-by-pixel distance between an image and its polygon decomposition. By computing the fitness drop of a decomposition when one polygon was removed, we had a measure of the impact of each polygon in the final reconstruction. We dub this measure visual information and report it normalized as a percentage. When running the BCI experiments we only used polygons with a visual information higher than 3% (15% during the calibration phase – see sec. 2.3.2). On average, the polygons eventually selected for the experiments bore a visual information of 13.5% with a standard deviation of 13.4%.

This visual information also allows us to rank the polygons within a decomposition according to their importance in the reconstruction. We used this ranking to select what target polygons are displayed in the initial bursts of the reconstruction, and we moved towards less informative polygons as the reconstruction proceeded, as explained in section 2.3.2.

Finally, in the oddball paradigm targets are displayed among allegedly neutral non-target stimuli. Whenever a picture was selected for reconstruction, the polygons in its decomposition were considered

target polygons. The polygons from the decomposition of all non-target images were held in a pool from which non-target polygons were drawn at the beginning of each burst (see appendix A.1 for discussion).

2.3.2 Experimental setup

The experiment consisted of a *calibration phase* and a *reconstruction phase* schematically depicted in figure 2. In either phase, a drawing from figure 1 was selected as a target and displayed for 5 seconds prior to each burst. A burst consisted on the rapid presentation of polygons that included target and non-target stimuli – i.e. primitives from the decomposition of the target and non-target images respectively. For each burst, 5 non-target polygons were selected for display together with the (one) corresponding target polygon.

A burst involves a number of blocks that may be different for the calibration and reconstruction phases. Each block consists of the display of all 6 polygons in a shuffled order. Each polygon is shown just once per block. The only constraint to the random order within a burst is that no primitive may appear twice in immediate succession. Because a burst is a series of blocks, this restriction only affects the randomness of a block given the last stimulus of the previous block. The SOA between successive polygons was 330 ms: during 230 ms it was shown the visual stimulus (the polygon) and during the last ms the corresponding polygon was substituted by a transparent rectangle – i.e. by a *void* stimulus.

Calibration phase: We restricted the visual stimuli to those polygons contributing more than 15% visual information. By avoiding polygons that might not be reliably appreciated as targets by the participant (due to little visual information), ERPs elicited by the target polygons were likely a valid signal to calibrate the classifier. Before each burst, a picture was selected as target image and one random polygon from its decomposition (among those with a visual information above 15%) was selected as target object. During this phase, a burst consisted of 4 blocks for subjects VPmao, VPmap, and VPjam; and of 10 blocks for any other subject. After each burst,

a new target image was selected. The subjects were told that, following the display of a drawing, random polygons would be presented and one or more of them could resemble the drawing or some salient feature of it. They were not explicitly instructed to seek for these stimuli in an active way. They were requested to avoid abrupt facial or any other movements and blinking, and to relax the jaw. Each ~ 15 minutes a self-paced pause was offered. During the calibration phase, there was no feedback provided to the participants.

Reconstruction phase: we considered all polygons from the decompositions that contributed more than 3%. For each subject, 15 reconstructions were completed. After choosing one of the drawings for reconstruction, it was displayed for 5 seconds. Then the first burst proceeded with the most informative polygon of the chosen drawing as target, together with 5 non-targets drawn from the pool of polygons. Bursts during this phase consisted of 4 blocks for subjects VPmai and VPmao, and 10 for any other subject. During each burst of the reconstruction phase, the classifier would score the likelihood that each polygon had elicited an ERP, and at the end of the burst, the primitive being most likely the target was determined, as explained in section 2.4. This primitive was displayed for 5 seconds as a feedback alongside the correct target polygon. Then the original target picture under reconstruction was shown again for 5 seconds and the next burst proceeded with the next more informative polygon as a target and with 5 new non-targets from the polygon pool. The correct stimuli from previous bursts were retained after they had been played out, so that the reconstruction could proceed. After a reconstruction was completed, a self-paced pause was offered. The instructions to the subjects were the same as during the calibration phase, only now they were explained that the reconstruction would proceed until a fair, schematic rendering of the target image had been reached. A video of a successful reconstruction is available [26].

2.4 Data analysis

ERP analysis: EEG signal were lowpass filtered with a Chebyshev filter using a passband up to 40 Hz

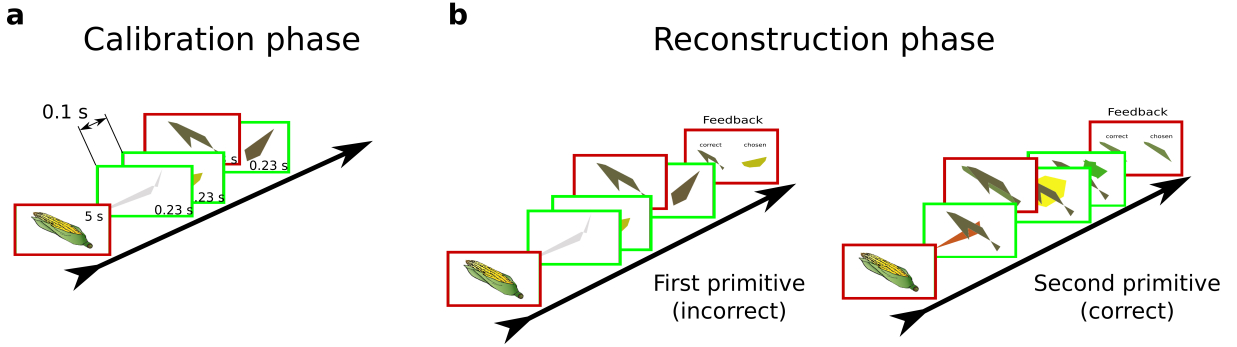


Figure 2: **Schematic representation of bursts during different phases of the experiment.** **a**, *calibration phase*. Bursts of polygons are presented to the subjects with no feedback between bursts. A target picture is randomly chosen for each burst. Stimuli in this phase are restricted to polygons bearing more than 15% visual information to ensure that ERPs are reliably elicited and measured. **b**, *reconstruction phase*. A target picture is chosen and remains target for several bursts until its reconstruction is completed. Each burst presents new target polygons upon the background where previous target primitives accumulate, thus implementing the image reconstruction. After each burst a feedback is provided showing the correct polygon and the polygon selected by the classifier. Despite the classification result, the correct polygon is always kept in successive bursts so that the reconstruction can proceed. An example of the reconstruction implemented is shown in [26].

and a stopband starting at 49 Hz, and then down-sampled to 100 Hz. Continuous signals were divided into epochs ranging from -200 ms to 1000 ms relative to each stimulus onset. Baseline correction was performed on the pre-stimulus interval of 200 ms. Epochs containing strong eye movements were detected and rejected using the following criterion: Epochs in which the difference of the maximum and the minimum values in one of the channels F9, Fz, F10, AF3, and AF4 exceeded $70 \mu\text{V}$ were rejected. Only those non-target epochs were used in which the three preceding and the three following symbols were also non-targets in order to avoid overlap from ERPs of preceding or successive targets. For the grand average the ERP curves were averaged across all trials and participants. To compare the ERP curves of two classes (*target* and *non-target*) signed r^2 -values were calculated.

Classification of what polygons the subject attended to: We employed binary classifiers based on spatio-temporal features. We sought for discrimination between epochs related to targets vs. non-targets. As preprocessing, EEG signals were down-sampled to 100 Hz by calculating the average for consecutive data points in non-overlapping stretches of 10 ms each. Epochs with an excessive power in a broadband ($5 - 40$ Hz) indicating, e.g., muscular artifacts were rejected from the calibration data. The aim of the heuristic is to find time intervals that have a stationary (target minus non-target difference) pattern and maximal r^2 differences. Occasionally the intervals determined by the heuristic were adjusted by the experimenter before starting the on-line runs. Features were calculated from 55 channels (all except for Fp1,2, AF3,4, F9,10, FT7,8) by averaging voltages within each of the five chosen time windows resulting in $55 \times 5 = 275$ dimensional feature vectors. For classification, a linear discriminant analysis (LDA) with shrinkage of the covariance matrix [27] was trained on calibration data. A polygon was determined by averaging the classifier output for all displayed polygons across the 4 or 10 blocks of each burst and choosing the primitive that received the largest averaged output.

In order to investigate the rate/accuracy trade-off the classifier that was used online was also applied

offline to the image reconstruction data, depending the polygon selection on averages across the first n blocks, with $n = 1, \dots, 10$. For $n = 10$ the same results as for online operation are obtained. For $n < 10$, an estimate of the potential performance when using a different number of blocks is achieved. We also computed the Information Transfer Rate per decision (ITR_d) – i.e. the number of bits involved in each classification – using:

$$ITR_d = \log_2(N) + p_c \log_2(p_c) + (1 - p_c) \log_2\left(\frac{1 - p_c}{N - 1}\right), \quad (1)$$

where $N = 6$ represents the number of primitives among which the classifier chooses and p_c represents the empirically measured probability of making the right classification [18, 28]. In the offline analysis, by normalizing over the number n of blocks for $n = 1, \dots, 10$ we get a proxy for the average number of bits that the classifier can extract per block in each possible scenario. Thus, we can trade off between the redundant information (offered by the repeated presentation of the same stimuli) and fast recovery (obtained by less presentations, but hindered by a lower accuracy). ITR_d approximates the amount of information extracted and can be overoptimistic, as noted in [18]. As an instance, it does not take into account the effect of corrections in the case that a wrong polygon is chosen by the classifier and incorporated to the canvas. We consider that it offers valuable information, though.

3 Results

3.1 ERPs

The ERP analysis of the data (figure 3) presents the grand average of brain activity over all subjects and trials under target and non-target stimuli. When plotting the scalp map of this activity (figure 3a) we readily appreciate how the ERPs of interest for our classification tasks are notable mainly in the frontal and central channels, being the occipital and temporal areas of null or little interest. This is consis-

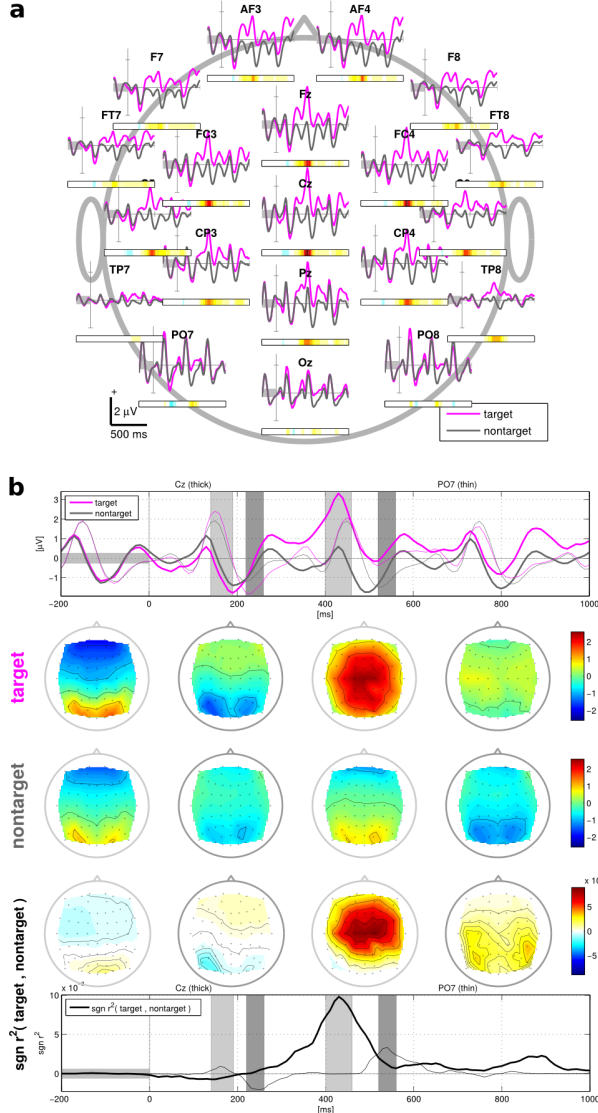


Figure 3: Event Related Potential analysis. Signals are averaged over all subjects and trials. **a** Average activity in different electrodes during target (magenta) and non-target (gray) stimulus presentation. **b** First row: averages over subjects of the potentials at channels Cz (thick) and PO7 (thin) during target and non-target trials. Shaded areas delimit important time intervals with notable divergences between signals associated to target and non-target stimuli. Second and third rows: brain activity averaged over each of these relevant time interval. Fourth and fifth rows: quantification of divergences between target and non-target signals with r^2 signed values distributed over the scalp and throughout time as a plot for the Cz and PO7 channels.

tent with the P300 ERP associated to the oddball paradigm.

For each subject, time intervals of interest have been selected to provide the classifier with discriminative data as it was indicated in section 2.4. In the grand average we can see how signals usually diverge between target and non-target activity (figure 3b) and what time intervals are more useful in average; the time interval between 400 and 500 ms being the most discriminative, which is once again consistent with the prominent role that the P300 ERP should play in the designed BCI.

3.2 Classification

During the reconstruction phase, the classification implemented after each burst was considered successful if the classifier had identified the corresponding target polygon from the current target drawing. This must be compared with approaches which have the experimental subjects reporting whether each stimulus is target or not. Note that a non-target stimulus might be considered target by a subject and ERPs might be elicited for such stimuli as well. That approach (considered, e.g. in [14], which reports very high classification accuracies) has not been taken here. This is further discussed in section 3.4.

The average online selection accuracy across all subjects is 73.4%. If we take into account only those subjects whose classification was based on bursts with 10 blocks, then the online selection accuracy raises to a 76.4%. This must be compared to the chance level for one target among 6 stimuli: 16.7%.

In an offline analysis we studied what would be the performance of the BCI if, within each burst, the classifier would consider less blocks to compute its output, as explained in section 2.4. The results are collected in figure 4. We appreciate a drop in performance for lower block number, as expected, but the averaged selection accuracy remains relatively high – above 60% for any choice with more than 4 blocks per burst (figure 4a).

Through the ITR_d normalized over the number of blocks we can trade off between accuracy and information redundancy (manifested as the time length of each burst) as explained in section 2.4. Because the

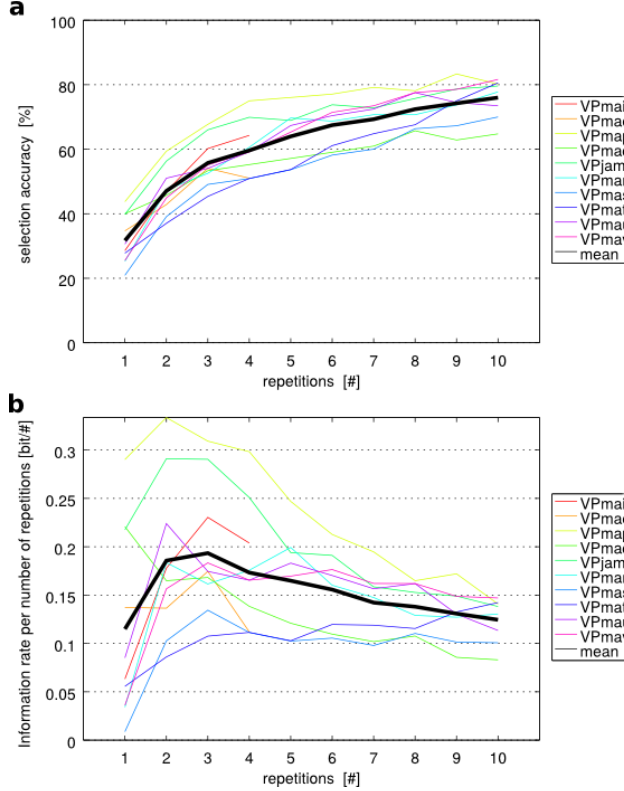


Figure 4: **Offline analysis of performance with alternative settings.** **a** It is possible to attain acceptable accuracies using less blocks per bursts. The accuracy grows less than linearly with the number of blocks. This suggests that an optimal operating point might exist at which a maximal accuracy could be reached faster. **b** IRT_d per number of blocks reveals a good operating point around 2 or 3 blocks per burst. This is a very optimistic results, but IRT_d and its approximative power is further diminished by the design of the experiment, which does not allow (and does not require either) for corrections over selected polygons.

accuracy grows slower than linearly with the number of blocks involved, there must be an optimal operating point. This is revealed around 2 or 3 blocks per burst in figure 4b, which is surprisingly (and positively) low. We must note once again that the IRT_d per number of blocks might be overoptimistic [18].

3.3 Performance drop with task difficulty

As indicated in section 2.3.2, during the reconstruction task a polygon is selected based on the output of the classifier. This might be the correct polygon – the one belonging to the target image reconstruction – or an incorrect one. Both the correct and the selected polygons are shown as a feedback to the subject and, whatever the outcome, the right polygon is held fixed on the background as new randomized stimuli are displayed in the following bursts. 25.3% of the paintings were completely reconstructed to its full extent without selecting any wrong polygon. This raises to 28.3% if we consider only subjects whose bursts consisted of 10 blocks. (The probability of reconstructing a picture by chance alone is lower than 0.001 even for the picture whose reconstruction consists of less polygons.) If we would consider the reconstructions only until the first wrong polygon is selected, a 49.9% (52.9% with 10 blocks) of the tasks would have been accomplished across subjects.

Because the right polygon was always preserved despite the outcome of the classifier, we could proceed with each reconstruction until the end and analyze the performance of the BCI as it explores more complicated scenarios in which target polygons convey very little information (down to 3%) about the target image. Thanks to this we can appreciate the selection accuracy drop for polygons bearing less visual information about the target (figure 5). Besides the obvious decay in accuracy for less informative primitives we observe an increase in heterogeneity. As we move towards a more difficult task it emerges a range of selection accuracies: some less informative polygons are rarely (two of them never) acknowledged as part of the target image while others are still correctly selected to a great extent. Polygons bearing more visual information tend to be accurately selected most

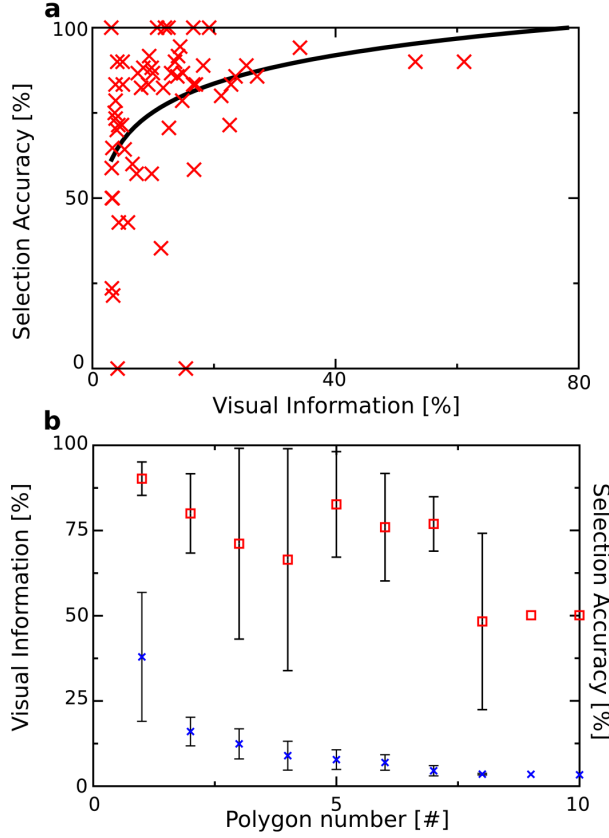


Figure 5: **Performance drop with task difficulty.** **a** Selection accuracy vs. visual information for individual polygons across subjects. Polygons bearing more information are usually larger, remind tightly in shape and color to their target, and are consequently easier to identify. Smaller polygons might reconstruct tiny details or refine existing shapes. These bear less visual information and represent a greater challenge for the image reconstruction, as indicated by the drop of performance for less information bearing polygons (thick, black trend line). It is remarkable, though, that a diversity of polygons with little visual info exists: some of them are correctly recognized almost always and others are definitely tough to classify for any subject. **b** Visual information (blue crosses) and selection accuracy (red squares) vs. rank that each polygon occupies in the reconstruction of its target. Error bars indicate standard deviation of the values across polygons. Polygons presented later convey less information and are consequently more difficult to recognize in average. However, there is a huge variability in selection accuracy and a marked drop around polygons 4 and 5. Both panels were elaborated using data from experiments with 10 blocks per burst. There is not any remarkable difference considering similar plots that include all data.

of time. Only 6 polygons have been always correctly selected, all of them carried a visual information below 20% and one of them is at the edge of the 3% threshold. These results were obtained for the 8 subjects with 10 blocks per burst during the reconstruction task. The outcome taking into account all subjects was broadly the same.

Less informative polygons happen later in the reconstruction task, as the experiment was designed and as we can appreciate in figure 5b. Consistently, the selection accuracy almost always decays as a reconstruction proceeds. Remarkably, the selection accuracy for the first polygon is 87.3% (90.8% for subjects with 10 blocks per burst). In figure 5b we also appreciate an unexpected drop (followed by a rise) of the selection accuracy for intermediate polygons. The reason for this is discussed in appendix B and lays on the particularly difficult task that polygons 3 or 4 of some reconstructions posed to the subjects.

3.4 Ambiguous polygons

In choosing our pictures for reconstruction we wanted them to be iconic with easily recognizable parts and with as few overlap as possible between them. But it cannot be avoided that some drawings (or parts of them) resemble each other. This led to an undesired effect during the experimental sessions: some polygons did not belong to the reconstruction of the target drawing, but they bore some resemblance to it and were often classified as target. Because these polygons are strictly non-targets, they were excluded from the selection accuracy results reported in section 3.2. This does not imply a malfunction of the classifier because such polygons could have tricked the subjects as well. These pieces introduce an interesting ambiguity as they could contribute to several reconstructions. We refer to them as *ambiguous polygons* later.

Based on how often each polygon was selected as a non-target, and how often this non-target was retrieved by the classifier for a given picture and across subjects; we computed the p -values to ascertain what polygons had been more probably not selected by chance alone, but presumably because an honest interference existed between these non-targets and the

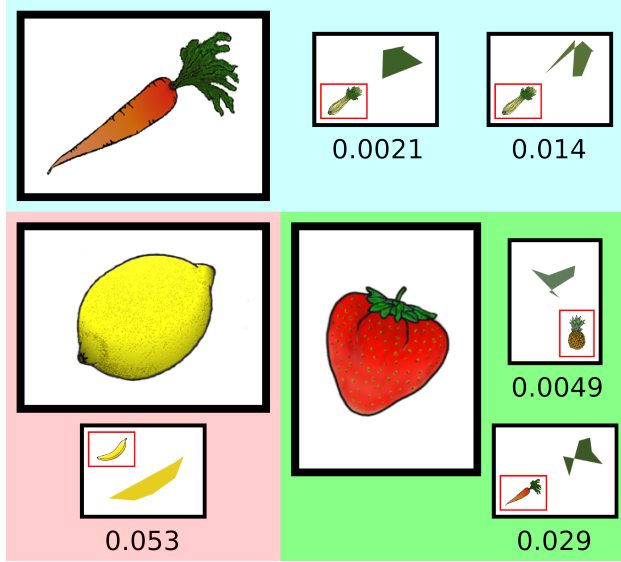


Figure 6: **Ambiguous polygons.** Some primitives could contribute to the reconstruction of different images. This could interfere with the reconstruction since these polygons would not be scored as correct classifications. The ambiguity of these pieces – that stems from the visual overlap between different targets – could be exploited to speed up the BCI image reconstruction. We shown the carrot, lemon, and strawberry together with some polygons that do not belong to their decompositions but that are overly selected by the classifier. For each polygon, within a red frame, it is shown the original drawing to which they belong. This figure was elaborated using data from experiments with 10 blocks per burst. The scenario is similar if we use all data for this analysis.

target drawing. We show the top 5 such pieces in figure 6 along with their p -values and the target images for which they were significantly over-selected. We appreciate that these could perfectly contribute to sketch the target – as the polygon from the banana in the case of the lemon reconstruction – or to the refinement of a smaller detail – as the green polygons seemingly selected to complete the leaves of the carrot and the strawberry. Furthermore, in these paradigmatic cases the wrongly classified non-targets would show up roughly in the same area as the actual target polygons.

4 Discussion

In this paper we show how Rapid Serial Visual Presentation using bursts of polygons together with the oddball paradigm is a working combination for BCI image reconstruction. Our purpose was merely to attain a proof of concept. For that end, different design choices have been made and tested during the experimental sessions. A systematic search of the best working settings was never intended and is left for future work. Notwithstanding this, the results reported in section 3 invite us to be optimistic about the paradigm and demand that further, more rigorous experiments are performed.

Explicitly, a series of aspects should be improved or carefully researched: i) The experimental settings; so that a faster, more reliable BCI can be built. ii) Advance towards a *free painting* BCI, to which different insights from this work could contribute – as we discuss below.

Concerning the experimental settings, the results from section 3.2 indicate a satisfactory performance with the relatively conservative (and tentative) parameters that we have chosen – meaning SOAs and other display options for the polygons. The number of blocks per burst are also an important aspect of the BCI design, as figure 4b shows. These results could serve as a guidance for further experiments if we choose to stick strictly to the setup presented here, but RSVP together with the oddball paradigm is very flexible and could allow the implementation of radically different approaches. Other experiments with

more audacious settings report good classification accuracy for RSVP similar tasks [11, 12, 14]. We have to be careful when translating these results because our paradigm is notably different.

If we wanted to move towards a RSVP-based free painting BCI machine we could exploit the existence of ambiguous primitives and we should consider seriously the necessity of error correcting mechanisms.

Regarding the correction of errors, in computing the IRT_d per number of blocks (section 3.2) we do not account correctly for the effect of wrongly classified stimuli. These wrong classifications would slow down our BCI if they needed to be removed or they could demand more polygons to correct whatever perturbation of the painting they create – so the effect of wrong polygons in the length of a reconstruction are not clear yet. This points at a partial explanation to the very optimistic results from figure 4b that suggest that ~ 2.5 blocks per burst is an optimal operating point. Other RSVP tasks contemplate mechanisms to correct for wrong outputs. In RSVP spellers a symbol can be explicitly incorporated among the letters to represent the backspace [19]. A similar approach could be taken for the present BCI application but it would likely interfere with the display of polygons. An appealing alternative are error potentials, a large scale signal elicited by unexpected feedback after a classification task, which can be used to automatically cancel incorrect selections that have been made by the classifier [29]. Furthermore, we note that for a free painting application the classification should also allow the ‘select nothing’ option for the case that none of the polygons that were selected for a burst would fit into the target image of the user.

Regarding ambiguous polygons, these are pieces that might contribute to the reconstruction of several different images as reported in section 3.2. This is so usually because the original drawings themselves share some common traits as in the case of the green leaves located around the same position for the carrot, the strawberry, etc (figure 5). They do not represent a generalized situation: it would just affect a few polygons, and scoring these cases as *correct* classifications would not change our selection accuracy sensibly.

For our results, these ambiguous polygons had a

negative effect because they do not count as correct classifications (and thus lower our selection accuracy); but in a wider scope they might be extremely useful. While we imposed that the image decomposition be unique for each drawing, we can conceive intermediate decompositions of multiple images with shared primitives. Then, a reconstruction should proceed from ambiguous, generalized descriptions towards more particular ones. This would establish a hierarchy that would cluster together pictures that are closer to each other in visual terms. By exploiting this feature we could discard non-targets quickly if they are very distant from our target. We should then research if the BCI protocol allows us to converge towards the target provided that successive primitives distinguish between each time closer images.

Linked to this, we could seek the use of maximally discriminating primitives at each reconstruction stage. Let us note the few constraints that we imposed upon the bursting polygons: many might be displayed within the same burst that convey redundant information, thus diminishing the exploratory capabilities of RSVP. How should we design our primitives to maximally exploit the BCI is one of the open research lines proposed for the future.

Acknowledgments

This work was supported in part by grants of the BMBF: 01GQ0850 and 16SV5839. The research leading to this results has received funding from the European Union Seventh Framework Programme (FP7/2007-2013) under grant agreement 611570. Seoane acknowledges the support of the Fundación Pedro Barrié de la Maza and useful discussion with members of the Complex Systems Lab, especially Sergi Valverde.

A Discussion of important design choices

A.1 Preprocessing of target images

We acknowledge both writing and painting as emergent processes, although at very different levels. While in the former minimal components are clearly identified (written characters, letters) the later is a truly emerging outcome of the very strongly, non-linearly interacting pieces that compose an image. It may be utterly complicated to come down to some basic components of a drawing. If we intend to produce a picture from scratch, our choice of building blocks (say our *alphabet* for drawing) could condition the complexity that can be generated, how difficult it is to render each picture, and how fast we can produce it. We need to find adequate primitives that can compose a range of images quickly by combining the minimal units. Our pieces should be simple and schematic, and as pivotal to our targets as letters are to writing. We think that this is an open problem. For this study we adopted a provisional solution that we describe in the following.

As targets for reconstruction we sought iconic images from the Snodgrass and Vanderwart’s object database [23]. The chosen pictures (figure 1) are drawings of fruits and vegetables with basic shapes and colors; all of them laid upon a white background, so that the reconstruction focuses in clear motives and not in peripheral details. Note anyway that the subject’s attention is free to wander over the screen. We discuss subject focus again in section A.2 in comparison with previous RSVP applications.

We needed to envision schematic, yet faithful, representations of the selected pictures. That was a preprocessing step completed weeks before the experiments. To extract useful primitives from our pool of drawings we found the perfect tool in recent applications of genetic algorithms (GAs) to image decomposition [24]. Such algorithms proceed through mutation and artificial selection from an arbitrary population of polygons to a set of polygons carefully arranged as to mimic a desired image.

For a GA, a fitness function needs to be introduced.

Take a set of random polygons laid upon a white background, and some upon each other – so there is a sense of depth. These compose an arbitrary image. Taken the RGB color scheme, we use as fitness function the pixel-by-pixel euclidean distance between the original picture and the image rendered by the collection of polygons. The better the fitness, the closer the collection of polygons resembles the original image.

As a seed for the algorithm we use an arbitrary collection of polygons $P_{i=0} = \{p_{0,j}; j = 1, \dots, n_j\}$, where i labels iterations and j labels the n_i polygons composing the collection. Note that n_i might change from one iteration to another. At each iteration the fitness of the current collection P_i is evaluated. Some mutations are applied to generate an alternative polygon composition P'_i . The collection with better fitness is retained: $\max_F\{F(P_i), F(P'_i)\} \rightarrow P_{i+1}$, where $F(\cdot)$ stands for the fitness function. The algorithm continues until a satisfactory convergence towards the original image has been reached or until the fitness does not improve for several iterations. The collection $P_{i_{end}}$ when the algorithm halts is referred to as the *polygon decomposition* of the original image.

The possible mutations applied at each iteration are: removal of a polygon or insertion of a new random one; swapping two polygons (recall that some polygons overlay some others); random addition, deletion, or modification of polygon’s vertexes; change of a polygon color. Details on the probability of each operation (provided along the code [25]) are not relevant as long as a satisfactory approximation of the original images is attained (which was done, as appreciated in figure 1).

The algorithm allows options regarding the kind of polygons that could be used. This turned out to be very important. We wished to discard very complex pieces, therefore only polygons with 3 to 7 vertexes were allowed. We did not use partially transparent polygons – as implemented by the α parameter in the RGB color scheme. This was a valid option for the original GA [24], but it introduced important non-linearities in the interactions between polygons. These effects could be difficult to grasp unless several correct pieces would fall into place at the same time, which our RSVP scheme did not allow. By using only opaque polygons we partially

solve this problem. Note however the complexity of the task under research. Emergent effects of several polygons cannot be discarded.

Once an image had been decomposed in its primitives, the fitness function also offered a measure of the importance of each piece in the reconstruction. For each polygon $p_j \in P_{i_{end}}$ we computed the fitness function of the whole arrange of polygons, and of the same arrange when p_j was removed. We defined the *visual information* carried by the polygon as the normalized drop in fitness. This is just a notation for this paper. There is not any intention of connecting this visual information to actual theoretical information measures. Along the paper we express this number as a percentage.

Using this visual information we ranked the polygons for each of our original images and retained only those contributing more than a 3% (or 15%, see section 2.3.2). This choice renders fine enough reconstructions (figure 1). Adding more polygons would only help with very tiny details and would make the experiments unnecessarily tedious.

The oddball paradigm requires that target stimuli are presented intermixed with neutral stimuli. When an original image from our pool was chosen as the object for reconstruction, all the polygons in its polygon decomposition became target stimuli. As for neutral stimuli, we used a pool containing all the polygons belonging to the decomposition of all other drawings.

This decision made the reconstruction task a fair one. All the polygons in our pool of neutral stimuli have been generated following the same procedure, only they belong to the polygon decomposition of different images. Differences between the two classes would ideally arise from their belonging or not to the target decomposition. If we would use, e.g., completely random polygons as neutral stimuli these could take any aspect, obviously including shapes that would hardly contribute to the generation of natural images. Such instances could be readily identified when opposed to polygons that account for details of some natural image. The reconstruction task would be artificially simplified by a preselection that greatly reduced the uncertainty about the tar-

get primitives. The task would effectively become a *recognition of the less random-looking polygon*.

A.2 Experimental setup

The natural guidelines for our BCI design are the experiments with RSVP spellers by Acqualagna and Blankertz [3, 4, 5]. These give us a remote idea of settings under which a BCI for image reconstruction could function. We chose rather conservative specifications, given the novelty of the procedure. As an instance, during RSVP burst a SOA of 330 ms between consecutive polygons was used. This lapse includes 100 ms during which a *void* stimulus was intercalated. These settings can be compared to the SOAs of 116 to 83 ms from [3, 4, 5], where letters succeeded each other without interspersing any voids. These differences (and the good results here and with RSVP spellers) suggest that there is room for improvement should we seek more ambitious experimental settings.

The original motivation to introduce RSVP to BCI spellers was that letters could be presented always at the focal point, which allows to exploit the enhanced brain signals prompted by on-focus stimuli. This is not an asset in our case: we must allow the subjects to focus on different areas of their visual field when peripheral details of the target images are being reconstructed. We did not impose any conditions on the focus of the subjects. Looking at the long term goals of this research the interest of RSVP would rather lay on its exploratory potential because of the random, combinatorial nature of the bursting primitives and its interplay with the subject’s (sub)conscious driving of the image reconstruction process. We are convinced that these ideas are worth exploring.

B Average performance drop for intermediate polygons

In section 3.3 it was reported the performance drop as the difficulty of the reconstruction task increased. Two approaches were taken: i) The selection accuracy was plotted against the visual information carried by each polygon and ii) the selection accuracy

was plotted as a function of the rank that each polygon occupied in the reconstruction. The first method asserts that the selection accuracy drops in average for polygons that contribute less to the reconstruction of the image (figure 5a). Highly informative polygons are usually correctly classified, but the least informative polygons display a great variety. Some of them are often well classified and some of them are not, with a range of selection accuracies in between. This indicates that the reconstruction task does not always become more difficult as we move towards less informative polygons.

Figure 5b reports the average selection accuracy across all reconstructions against the rank that a given polygon occupies in the reconstruction. The reconstruction task proceeds from the most informative polygons to the less informative ones, given the target picture. The later bear less information about the original image, thus it should become more difficult to classify them correctly. Unexpectedly, the decay in performance is not a monotonous function: polygons 5, 6, and 7 in the reconstruction are selected with notably more accuracy than polygons 3 and 4. This indicates that there are some less informative polygons that are correctly selected more often than the average of other, more informative polygons.

Figure 7 clarifies this drop in performance for intermediate polygons. When we look at the average accuracy per polygon for single reconstructions we note that some of them present a strongly marked fall in selection accuracy for polygons 3 and 4: the strawberry in polygon 3; and the carrot, the pear, and the pineapple in polygon 4. All four cases present a selection accuracy lower than 50% for these polygons, contributing to an average performance drop across reconstructions. These polygons happen to be just difficult to classify.

In two of these cases (strawberry and pear) the problematic polygons are very light gray pieces that contribute to the reconstruction (perhaps by occluding some spurious detail brought in by earlier pieces, as with the third polygon of the cherry [26]). Because they are almost white, they are easy to miss against the blank background. In the case of the carrot the performance drop is not so dramatic. Also, this polygon number 4 contributes to the leaves of

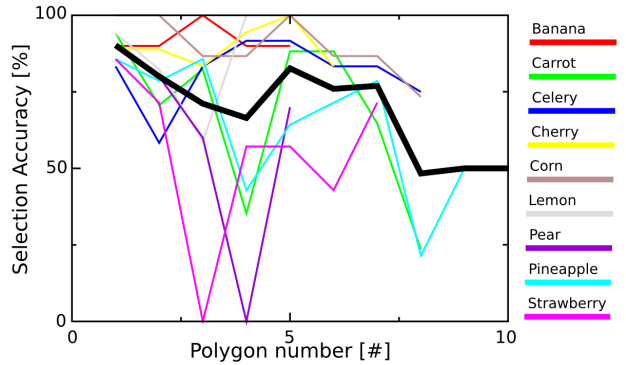


Figure 7: Performance drop in early polygons. Polygons appearing earlier in the reconstruction task bear more visual information about the targets than those showing up later. The former should be easier to recognize and be correctly classified more often. Despite this, there is a marked drop in selection accuracy of intermediate polygons when accuracy is averaged over all polygons with the same rank in the distribution (black thick line). We appreciate that the strawberry (magenta), the carrot (green), the pear (violet), and the pineapple (cyan) pose challenging tasks to the subjects precisely at polygons 3 or 4 of their decomposition, accounting for the average drop.

the carrot and, as we saw in section 3.4, that was precisely a common location of ambiguous polygons. If some ambiguous non-targets have been overly misclassified, some actual targets must necessarily be missed.

Nothing remarkable has been recognized in the case of the pineapple: the conflicting polygon seems to be a working, non-ambiguous piece of the reconstruction and we just assume that this precise primitive was more difficult for the subjects (note that the performance raises back to average for polygons 6 and 7 of the pineapple). Among the four important deviations at intermediate stages, this is the case with the lowest drop.

References

- [1] Patel SH and Azzam PN (2005). Characterization of N200 and P300: selected studies of the event-related potential. *Int. J. Med. Sci.* **2**, 147-154.
- [2] Polich J (2007). Updating P300: an integrative theory of P3a and P3b. *Clin. Neurophysiol.* **118**, 2128-2148.
- [3] Acqualagna L and Blankertz B (2010). A novel brain-computer interface based on the rapid serial visual presentation paradigm. *Conf. Proc. IEEE Eng. Med. Biol. Soc.*, 2686-2689.
- [4] Acqualagna L and Blankertz B. A gaze independent spelling based on rapid serial visual presentation. *Conf. Proc. IEEE Eng. Med. Biol. Soc.*, 2011.
- [5] Acqualagna L and Blankertz B (2013). Gaze-independent BCI-spelling using rapid serial visual presentation (RSVP). *Clin. Neurophysiol.* **124**, 901-908.
- [6] Gerson AD, Parra LC, and Sajda P (2006). Cortically-coupled computer vision for rapid image search. *IEEE Trans. Neural Syst. Rehabil. Eng.* **14**, 174-179.
- [7] Parra LC, Christoforou C, Gerson AD, Dyrholm M, Luo A, Wagner M, Philistiades MG, and Sajda P (2008). Spatiotemporal linear decoding of brain state: application to performance augmentation in high-throughput tasks. *IEEE Signal Process. Mag.* **25**, 95-115.
- [8] Sajda P, Pohlmeier E, Wang J, Parra LC, Christoforou C, Dmochowski J, Hanna B, Bahlmann C, Singh MK, and Chang S-F (2010). In a blink of an eye and a switch of a transistor: cortically coupled computer vision. *Proc. IEEE* **98**, 462-478.
- [9] Bigdely-Shamlo N, Vankov A, Ramirez RR, and Makeig S (2008). Brain activity-based image classification from rapid serial visual presentation. In *Neural Systems and Rehabilitation Engineering, IEEE Transactions on*, **16**(5), 432-441.
- [10] Huang Y, Erdogmus D, Pavel M, Mathan S, and Hild II KE (2010). A Framework for Rapid Serial Visual Image Search using Single-trial Evoked Responses. *Neurocomputing* **74**(12), 2041-2051.
- [11] Pohlmeier EA, Wang K, Jangraw DC, Lou B, Chang S-F, and Sajda P (2011). Closing the loop in a cortically-coupled computer vision: a brain-computer interface for searching image databases. *J. Neural Eng.* **8**, 036025.
- [12] Ušćumlić M, Chavarriaga R, and Millán JdR (2013). An Iterative Framework for EEG-based Image Search: Robust Retrieval with Weak Classifiers. *PLoS one* **8**(8), e72018.
- [13] Basa T, Go CA, Yoo K-S, and Lee W-H (2006). Using Physiological Signals to Evolve Art. In *Applications of Evolutionary Computing* (pp. 633-641). Springer Berlin Heidelberg.
- [14] Shamlo NB and Makeig S (2009). Mind-Mirror: EEG-Guided Image Evolution.

- Novel Interaction Methods and Techniques (pp. 569-578). Springer Berlin Heidelberg.
- [15] <http://www.picbreeder.com>
- [16] Kübler A, Halder S, Furdea A, and Hösle A (2008).
“Brain Painting – BCI meets art”,
in Proceedings of the 4th International Brain-Computer Interface Workshop and Training Course, 361-366.
- [17] Halder S, Furdea A, Leeb R, Müller-Putz G, Hösle A, and Kübler A (2009).
“Implementation of SMR based brain painting”,
in Poster at Neuromath Workshop. Leuven, Belgium.
- [18] Müsinger JI, Halder S, Kleih SC, Furdea A, Raco V, Hösle A, and Kübler A (2010).
Brain Painting: First Evaluation of a New Brain-Computer Interface Application with ALS-Patients and Healthy Volunteers.
Front. Neurosci. **4**, 182.
- [19] Farwell LA and Donchin E (1988).
Talking off the top of your head: toward a mental prosthesis utilizing event-related brain potentials.
Electroencephalogr. Clin. Neurophysiol. **70**, 510.
- [20] Venthur B, Scholler S, Williamson J, Dähne S, Treder MS, Kramarek MT, Müller K-R, and Blankertz B (2010).
Pyff—A Pythonic Framework for Feedback Applications and Stimulus Presentation in Neuroscience.
Frontiers Neurosci. 00179, doi: 10.3389/fnins.2010
- [21] <http://www.pygame.org>
- [22] Straw AD (2008).
Vision Egg: An Open-Source Library for Real-time Visual Stimulus Generation. *Frontiers Neuroinformatics*, doi: 10.3389/neuro.11.004.2008
- [23] Rossion L and Pourtois G, Revisiting Snodgrass and Vanderwart’s object database: Color and Texture improve Object Recognition. *J. of Vision* (2001).
- [24] <http://alteredqualia.com/visualization/evolve/>
<https://code.google.com/p/alsing/downloads/list>
- [25] https://github.com/dedan/poly_burst
- [26] <http://youtu.be/LERyK3z2cYs>
- [27] Lemm S, Blankertz B, Dickhaus T, and Müller KR (2011).
Introduction to machine learning for brain imaging.
Neuroimage **56**(2), 387-399.
- [28] McFarland DJ and Wolpaw JR (2003).
EEG-based communication and control: Speed-accuracy relationships. *Appl. Psychophysiol. Biofeedback* **28**(3), 217-231.
- [29] Schmidt N, Blankertz B, and Treder MS (2011).
Online detection of error potentials increases information throughput in a brain-computer interface.
Neurosci Lett, **500**(1), 19-20.